

MICROCOPY

CHART

MRC Technical Summary Report #2915

ZERO AND NEGATIVE MASSES IN FINITE
ELEMENT VIBRATION AND TRANSIENT
ANALYSIS

David S. Malkus and Michael E. Plesha

AD-A167 489

Mathematics Research Center
University of Wisconsin—Madison
610 Walnut Street
Madison, Wisconsin 53705

February 1986

(Received October 24, 1985)

DTIC FILE COPY

DTIC
ELECTE
MAY 23 1986
S D

Approved for public release
Distribution unlimited

Sponsored by

U. S. Army Research Office
P. O. Box 12211
Research Triangle Park
North Carolina 27709

86 5 20 138

April 30, 1986

Errata to:

MRC Technical Summary Report #2915

Zero and Negative Masses in Finite Element Vibration and Transient Analysis

David S. Malkus and Michael E. Plesha

page 1, paragraph 2	negative should be negative
page 9, paragraph 1	$0 \leq i \leq \dots$ should be $1 \leq i \leq \dots$
page 16, equation (37)	last term in equation should be postmultiplied by $\{\bar{V}^E\}$ instead of $\{\hat{V}^E\}$
page 16, equation (40)	$4/\Delta t^2$ should be $\Delta t^2/4$
page 18, paragraph 5	last sentence: reference to equation (46) should be to equation (47)
page 21, paragraph 2	an viable should be a viable
page 22	somes sense should be some sense
Section 6	following references on original work in partitioned transient analysis should be added: T. Belytschko and R. Mullen, Mesh Partitions of Explicit-Implicit Time Integration, in Formulations and Computational Algorithms in Finite Element Analysis, K. J. Bathe, et al eds., MIT Press, 1976. T. Belytschko and R. Mullen, Stability of Explicit-Implicit Mesh Partitions in Time Integration, Int'l. J. Numerical Methods in Engr., 12, 1575-1586 (1978).

NOTE: This report will be published in substantially the same form in Computer Methods in Applied Mechanics and Engineering.

UNIVERSITY OF WISCONSIN-MADISON
MATHEMATICS RESEARCH CENTER

ZERO AND NEGATIVE MASSES IN FINITE ELEMENT VIBRATION
AND TRANSIENT ANALYSIS

David S. Malkus* and Michael E. Plesha**

Technical Summary Report #2915

February 1986

ABSTRACT

Mass matrix lumping by quadrature is considered. Accuracy requirements seem to dictate the use of zero or negative masses for multi-dimensional higher-order elements. It is shown that the zero and/or negative masses do not destroy the essential algebraic properties of the discrete eigenproblem, in spite of the negative or infinite eigenvalues which may result. Explicit transient methods require positive definite lumping which, for some elements, may only be achieved by sacrificing accuracy to avoid the negative or zero masses that would render the lumping indefinite. An implicit-explicit time integration method based on quadratic triangles with optimal lumping is devised, analysed, and tested. It treats the nodes with nonzero masses explicitly and the nodes with zero masses implicitly. Analysis and numerical tests show that this formulation is optimally accurate and less costly than a similar method with nonzero masses, based on optimally lumped biquadratic rectangles. The method is also found to be substantially more accurate than the fully explicit method based on lumping the triangular elements in an ad-hoc fashion to retain non-zero masses.

AMS (MOS) Subject Classifications: 65N05, 65N25, 65N30, 73K25

Key Words: Explicit, Finite element, Implicit, Lumping, Mass matrix;
Numerical quadrature; Stability, Time integration, Vibration modes

Work Unit Number 3 (Numerical Analysis and Scientific Computing)

*Mathematics Research Center and Engineering Mechanics Dept., University of Wisconsin-Madison, Madison, WI 53705.

**Engineering Mechanics Dept., University of Wisconsin-Madison, Madison, WI 53706.

Sponsored by the United States Army under Contract No. DAAG29-80-C-0041.

ZERO AND NEGATIVE MASSES IN FINITE ELEMENT VIBRATION AND TRANSIENT ANALYSIS

David S. Malkus* and Michael E. Plesha**

1. INTRODUCTION

Mass matrix lumping is a technique in finite element transient and vibration analysis whereby the banded, symmetric, positive definite matrix representing the L_2 inner product (i.e., the consistent mass matrix) is replaced by a diagonal matrix which is in some sense equivalent. This is done for two basic purposes: first, to make truly explicit finite element transient analysis possible, and second to save computer storage space and operations in the solution of eigenproblems associated with the finite element vibration problem. There are two additional benefits associated with lumped masses: in transient analysis, lumping lowers the highest wave speed in the mesh significantly, with an attendant raising of the critical time step for explicit integration schemes; in eigenanalysis, lumping removes the strict upper-bounding of the discrete eigenvalues. The result can be that the eigenvalues remain optimally accurate in terms of convergence rate, but have a better constant in the error bound.

The role of lumping in transient analysis makes it an essential tool in finite element analysis. Many problems in structural analysis are nonlinear hyperbolic problems which can be treated explicitly. The geometric complexity of many practical problems, such as in reactor technology requires so many finite elements that any fully implicit treatment of the nonlinearity would be impractical. Thus the basic idea behind lumping stems from practical necessity and has a ready physical interpretation: the continuous distribution of mass in the body is replaced by one in which the mass is concentrated at the nodal points. That this has the desired effect on the mass matrix can easily be seen by replacing the mass density function by the sum of delta functions with support at the nodes. For low-order elements, the requirements of preserving the total mass of the element and respecting the symmetry of the distribution about natural axes of the element uniquely determines the lumped distribution. For higher-order elements, many distributions seem to respect natural symmetry, but most seem to lead to schemes with reduced accuracy.

An approach to recovering optimal accuracy with lumping schemes is to require each element to exactly reproduce as many moments of the mass distribution as possible. This turns out to be equivalent to the use of a nodally based quadrature formula to evaluate the L_2 inner product. This is the fundamental observation of ref. 1. Once we recognize that lumping and numerical quadrature correspond, then we can be guided by the error analysis of the latter in devising lumping schemes. Here we consider only second-order problems, and in that case, ref. 1 argues that we should choose a nodal formula of degree of precision $2p - 2$ where p is the degree of the maximal complete polynomial on each

*Mathematics Research Center and Engineering Mechanics Dept., University of Wisconsin-Madison, Madison, WI 53705.

**Engineering Mechanics Dept., University of Wisconsin-Madison, Madison, WI 53706.

Sponsored by the United States Army under Contract No. DAAG29-80-C-0041.



Codes	
Dist	Avail and/or Special
A-1	

element. When that is done, the error introduced by quadrature will be bounded by $Ch^p \|u\|_{p+1}$ and thus be on the same order as the overall error of the scheme, and no accuracy will be lost.

One quickly finds that the degree of precision requirement for retaining optimal accuracy is not a trivial one. In fact, for elements with $p \geq 3$, the traditional equal spacing of nodes in the reference element will no longer suffice [1]. A multidimensional generalization of Lobatto [2] integration is called for; vertex nodes must be included, and boundary nodes must remain on boundaries, but the nodal locations must be chosen so as to otherwise maximize the degree of precision [1]. For one-dimensional problems, the Lobatto weights can be shown to be positive [2]. This is important, since in all dimensions the quadrature weights are the diagonal entries of the lumped mass matrix. But in two or more dimensions, a fundamental difficulty in numerical analysis arises: maintaining positive weighting and specifying quadrature point locations can be mutually exclusive. Two-dimensional elements for which this conflict occurs are schematically illustrated in Figure 1. The appearance of zero and negative weights seems to leave the practitioner four choices: (1) use low order elements, (2) use elements which are tensor products of one dimensional elements, (3) use lumping schemes which sacrifice degree of precision to the maintenance of positive weights, or (4) employ a non-positive-definite mass matrix with coefficients that can be positive, zero or negative. The purpose of this paper is to demonstrate that (4) is a viable computational alternative.

2. THE NONPOSITIVE MASS PROBLEM

There appear to be at least three difficulties with nonpositive mass lumpings, beyond the obvious physical peculiarity. Actually, the physical peculiarity cannot be a particularly serious problem, because the lumping scheme is devised to produce optimally accurate eigenvalues. Their presence in the spectrum and their accuracy can thus be guaranteed a-priori, and any other modes present in the problem must take their place within the unphysical portion of the spectrum, which is there whether or not the masses are lumped. But there are a number of possible technical difficulties. In eigenanalysis, zero masses are known not to be problematical, and can in fact be put to good use in static condensation [3]. But in transient analysis zero masses seem to defeat the very purpose of lumping. An explicit multistep method would have the form

$$[M]\{D_n\} = \{\mathcal{F}(\{D_{n-1}\}, \{D_{n-2}\}, \dots, \{D_{n-k}\}, \{F_{n-1}\})\} \quad (1)$$

Clearly no unique solution can exist when $[M]$ is singular, even if diagonal. Negative masses seem even more troublesome. The finite element eigenproblem

$$[K]\{D\} = \lambda[M]\{D\} \quad (2)$$

could have negative eigenvalues when $[M]$ is indefinite. For statically well-determined problems we shall presume $[K]$ is positive definite. In that case it is clear that there will be as many negative eigenvalues as negative masses. However, for free body vibrations, $[K]$ is singular. In such a case there may or may not be negative eigenvalues when $[M]$ has negative entries. One cannot be sure a-priori because when $[M]$ is indefinite and $[K]$

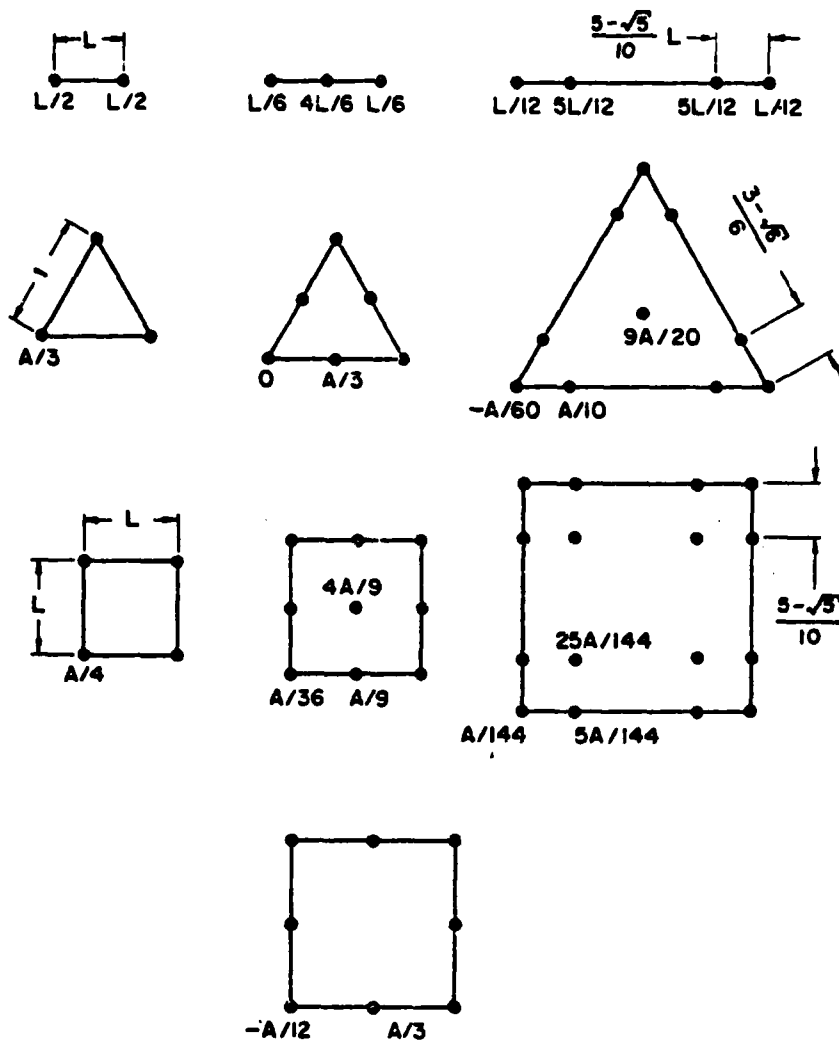


FIGURE 1

Optimal lumpings for some common 1- and 2-D elements. Triangular elements are equilateral reference elements in area coordinates. Complete symmetry of lumping formula in area coordinates is assumed, determining nodal locations and unspecified weights completely from given information. Square elements are isoparametric master elements. Complete symmetry in Cartesian coordinates uniquely determines lumping formulas. "A" denotes area of 2-D elements.

is singular, the fundamental structure of the eigensystem can be quite different from the case in which either matrix is positive definite. A simple example:

$$[K] = \begin{bmatrix} 1 & -1 \\ -1 & 1 \end{bmatrix}, [M] = \begin{bmatrix} -1 & 0 \\ 0 & 1 \end{bmatrix}$$

Let

$$[P] = \begin{bmatrix} 1 & -2 \\ -1 & 1 \end{bmatrix}, [Q] = \begin{bmatrix} 1 & -2 \\ 1 & -1 \end{bmatrix}$$

Then the matrix pencil $[K] - \lambda[M]$ is equivalent to [4]

$$[P]([K] - \lambda[M])[Q] = \begin{bmatrix} -\lambda & 1 \\ 0 & -\lambda \end{bmatrix} \quad (3)$$

We therefore have a multiple zero eigenvalue and a nonlinear divisor. No negative eigenvalues exist, and the matrix pencil is no longer diagonalizable. Examples can be constructed in which the eigenvalues are complex. Even worse, if there are zero masses, examples can be found in which there fails to be a complete set of eigenvalues [4]. The simplest way this can happen is for $[K]$ and $[M]$ to have a common null-space.

The above example is clearly contrived. It would not arise in finite element analysis; $[K]$ is a simple stiffness matrix for a linear element, but the mass matrix is lumped in a way that does not preserve mass. To put it another way, the quadrature formula whose weights are the diagonal entries would violate the degree of precision requirement: the degree of precision is not even zero, whereas $2p - 2 = 0$. The fear in using negative masses is that, while quadrature accuracy may force the existence of accurate eigenvalues, they may be tied up in nonlinear divisors, have the wrong multiplicity, and be hard to compute. There could conceivably be negative eigenvalues of the same magnitude of the accurate eigenvalues leading to spurious, unstable, low frequency modes.

The first task to which we turn our attention is to generalize what we observed in the simple example, the fact that preservation of mass and higher moments of mass rules out the pathologies. But this is easier to tackle in an equivalent form; satisfaction of the degree of precision requirement rules out all the difficulties allude to above.

3. MASS MATRIX LUMPING BY QUADRATURE

We shall deal with second-order, self-adjoint problems in which the natural modes of the exact problem make the Rayleigh quotient, $Q(\mathbf{u})$, stationary,

$$Q(\mathbf{u}) \equiv \frac{a(\mathbf{u}, \mathbf{u})}{b(\mathbf{u}, \mathbf{u})} \quad (4)$$

where $a(\cdot, \cdot)$ represents the strain energy, $b(\cdot, \cdot)$ represents the L_2 inner product, and for some real γ

$$a(\mathbf{u}, \mathbf{u}) \geq \gamma^2 \|\mathbf{u}\|_1^2$$

for $\mathbf{u} \in H_{E_1}^1 \times H_{E_2}^1 \times H_{E_3}^1 = H$. $H_{E_i}^1$ denotes the space of functions with square integrable first partials satisfying essential boundary conditions appropriate to the i^{th} vector component of the solution. For plane or 1 - D problems, from which our examples are drawn, we

may consider that $H_{E_i}^1 = 0$ for one or two factors of the trial space. Generalization of our results and examples to 3 - D is straight-forward.

It will be convenient here to use fairly standard engineering finite element notation [3]; $u \in H$ will be approximated in element "e" by

$$u^h|_e = [N_e] \{d\} \quad (5)$$

where $\{d\}$ represents the nodal-value degrees of freedom and $[N_e]$ is the element shape-function matrix which has the form

$$[N_e] = \begin{bmatrix} N_{1e} & 0 & \dots & N_{me} & 0 \\ 0 & N_{1e} & \dots & 0 & N_{me} \end{bmatrix} \quad (6)$$

for an m-noded element in 2 - D. Generalizations to 1 - and 3 - D problems are obvious. Note that equation (6) implies a nodal ordering in which the degrees of freedom associated with a given node are grouped together in $\{d\}$ [3]. Element shape functions are pieced together in the usual manner to produce a global nodal representation

$$u^h = [N] \{D\} \quad (7)$$

where

$$[N] = \begin{bmatrix} N_1 & 0 & \dots & N_M & 0 \\ 0 & N_1 & \dots & 0 & N_M \end{bmatrix} \quad (8)$$

which illustrates the M-noded, 2 - D case. Satisfaction of the essential boundary conditions in equation (7) is assumed to be accomplished by specification of appropriate entries of $\{D\}$ to prescribed values [3].

The free-structure stiffness matrix is assembled from element matrices

$$[k_e] = \int_e [B_e]^T [E] [B_e] dV \quad (9)$$

where $[E]$ is a symmetric matrix of material coefficients and

$$[B_e] = [D] [N_e] \quad (10)$$

$[D]$ is a matrix of first-order partial differential operators relating stress to strain (or strain-rate in fluid problems). For example, in plane elasticity

$$[D] = \begin{bmatrix} \frac{\partial}{\partial x} & 0 \\ 0 & \frac{\partial}{\partial y} \\ \frac{\partial}{\partial y} & \frac{\partial}{\partial x} \end{bmatrix} \quad (11)$$

Boundary conditions implied by $H_{E_i}^1$ are assumed to be homogeneous and are enforced by omission of corresponding rows and columns during assembly [3]. Entries in the global nodal-value vector, $\{D\}$, are omitted along with corresponding columns in $[N]$. The space

of all such functions defined by equation (7) is denoted by S^h . The global stiffness matrix, possibly dimensionally reduced by imposing boundary conditions, is

$$[K] = \int_{\Omega} [B]^T [E] [B] dV \quad (12)$$

where

$$[B] = [D] [N] \quad (13)$$

For future reference in dynamic problems we note that

$$\begin{aligned} \{d\}^T [k_e] \{d\} &= \int_e \{\sigma_e\}^T \{\epsilon_e\} dV \\ \{\epsilon_e\} &\equiv [B_e] \{d\} \\ \{\sigma_e\} &\equiv [E] [B_e] \{d\} \end{aligned} \quad (14)$$

and

$$\begin{aligned} \{D\}^T [K] \{D\} &= \int_{\Omega} \{\sigma\}^T \{\epsilon\} dV \\ \{\epsilon\} &\equiv [B] \{D\} \\ \{\sigma\} &\equiv [E] [B] \{D\} \end{aligned} \quad (15)$$

Equations (14) and (15) give the virtual work done against internal stresses by the displacements. The matrix of $a(\cdot, \cdot)$ in equation (4) is $[K]$. With no essential boundary conditions, $\gamma = 0$.

The mass matrix gives the matrix of $b(\cdot, \cdot)$ in equation (4) and is defined on the element and global level by

$$\begin{aligned} [m_e] &= \int_e \rho [N_e]^T [N_e] dV \\ [M] &= \int_{\Omega} \rho [N]^T [N] dV \end{aligned} \quad (16)$$

where ρ is the material's mass-density function. In what follows, ρ may be non-constant, but $\rho > 0$ is assumed. When the integrations in equation (16) are exact, $[m_e]$ and $[M]$ are called "consistent". To lump the mass matrix by quadrature, the nodes are located in order to maximize the degree of precision of a nodal quadrature formula, while retaining interelement compatibility [1], and equation (16) is integrated with the nodal quadrature

rule, resulting in

$$\begin{aligned}
 [\tilde{m}_e] &= \sum_{i=1}^m \rho_i w_i J_i \begin{bmatrix} 0 & 0 \\ 0 & 0 \\ \vdots & \vdots \\ 1 & 0 \\ 0 & 1 \\ \vdots & \vdots \\ 0 & 0 \\ 0 & 0 \end{bmatrix} \begin{bmatrix} 0 & 0 & \dots & 1 & 0 & \dots & 0 & 0 \\ 0 & 0 & \dots & 0 & 1 & \dots & 0 & 0 \end{bmatrix} \\
 &= \begin{bmatrix} \rho_1 w_1 J_1 [I_2] & & & & & & & \\ & \rho_2 w_2 J_2 [I_2] & & & & & & \\ & & \ddots & & & & & \\ & & & 0 & & & & \\ & & & & \ddots & & & \\ & & & & & 0 & & \\ & & & & & & \rho_m w_m J_m [I_2] & \end{bmatrix}
 \end{aligned} \tag{17}$$

where, again, an m -noded 2-D element illustrates the generality; ρ_i and J_i are evaluations of the density and any isoparametric or curvilinear Jacobian implied in " dV " at the element nodes, respectively, and the w_i are the quadrature weights. $[I_2]$ is the 2×2 identity. In this notation superposed tilde denotes quantities evaluated by numerical quadrature. Clearly the $[\tilde{m}_e]$ can be assembled into a global, lumped mass matrix, $[\tilde{M}]$, which is diagonal.

4. LUMPING AND EIGENSTRUCTURE

The basic result we use to investigate the effect of lumping on the pencil $[K] - \lambda[\tilde{M}]$ is that of G. Fix [5], which deals with the accuracy of applying a quadrature formula to equations (9) and (16) (on the element level) to produce numerically integrated forms $\tilde{a}(\cdot, \cdot)$ and $\tilde{b}(\cdot, \cdot)$ when numerically integrated stiffness and mass matrices are assembled. The analysis applies to lumping by quadrature. The major result is based on the satisfaction of two conditions:

(A) Stability: Let $\mathbf{u}^h, \mathbf{v}^h \in S^h$

$$\sup_{\|\mathbf{u}^h\|_H = \|\mathbf{v}^h\|_H = 1} |c(\mathbf{u}^h, \mathbf{v}^h) - \tilde{c}(\mathbf{u}^h, \mathbf{v}^h)| \rightarrow 0 \tag{18}$$

(B) Accuracy: Let $\mathbf{u}^h \in S^h$ be a finite element eigenfunction and $\mathbf{v}^h \in S^h$

$$\sup_{\|\mathbf{v}^h\|_H = 1} |c(\mathbf{u}^h, \mathbf{v}^h) - \tilde{c}(\mathbf{u}^h, \mathbf{v}^h)| \leq \delta_c^h(\mathbf{u}^h) \tag{19}$$

where $c(\cdot, \cdot)$ denotes $a(\cdot, \cdot)$ or $b(\cdot, \cdot)$, and h is the mesh parameter, typically the maximal element diameter.

Let $\hat{\mathbf{u}}^h$ denote eigenfunctions which are stationary points of

$$\hat{Q}(\mathbf{u}) \equiv \frac{\tilde{a}(\mathbf{u}^h, \mathbf{u}^h)}{\tilde{b}(\mathbf{u}^h, \mathbf{u}^h)} \tag{20}$$

Clearly α_i, β_i are real and $\alpha_i > 0$. Assume the ordering is such that the k zero β_i are ordered first, so $\beta_i = 0, 0 \leq i \leq k \leq n$. A few simple facts should be apparent:

- (1) The eigenvalues are $\alpha_i/\beta_i, k < i \leq n$ and ∞ (k times).
- (2) If λ_0 is any real number, the eigenvalues of $[K] - (\lambda - \lambda_0)[\tilde{M}]$ are $\alpha_i/\beta_i + \lambda_0, k < i \leq n$ and ∞ (k times).

We now turn our attention to the case in which $[K]$ has rigid body modes and is only semi-definite.

Lemma: Let Condition (A) hold for the lumping formula. Given any $\lambda_0 > 0$, there is an h sufficiently small such that for all $h < h_0$, $[K] - \lambda_0[\tilde{M}]$ is positive definite.

Proof: $[K] + \lambda_0[M]$ is a positive definite stiffness matrix. $[K] + \lambda_0[\tilde{M}]$ is a stable quadrature evaluation of the consistent matrix. Stability implies the existence of a $\tilde{\gamma}$ such that

$$\tilde{a}(\mathbf{u}, \mathbf{u}) + \lambda_0 \tilde{b}(\mathbf{u}, \mathbf{u}) \geq \tilde{\gamma}^2 \|\mathbf{u}\|_H^2$$

Theorem 1: For sufficiently small h there exists $[Q]$ as in equation (22) diagonalizing the pencil $[K] - \lambda[\tilde{M}]$ whether $[K]$ is positive definite or semi-definite, whenever the lumping quadrature is stable.

Proof: Pick any $\lambda_0 > 0$. Let h be sufficiently small so that $[K] + \lambda_0[\tilde{M}]$ is positive definite. Equation (22) applies to $([K] + \lambda_0[\tilde{M}]) - \lambda[\tilde{M}] = [K] - (\lambda - \lambda_0)[\tilde{M}]$. As observed above, reshiftng by $-\lambda_0[\tilde{M}]$ does not change the eigenstructure and results in $[K] - \lambda[\tilde{M}]$.

Remarks:

- (1) Since λ_0 can be arbitrarily small in Theorem 1, it is no surprise that in practice the result is observed to hold without making h small and even to hold for one element.
- (2) Theorem 1 says that the divisors of the pencil $[K] - \lambda[\tilde{M}]$ are linear and furthermore the pencil is diagonalizable by $[\tilde{M}]$ -orthogonal transformations.
- (3) $[Q]^T[\tilde{M}][Q]$ has the same signature as $[\tilde{M}]$, so that the number, k , of zero β_i is the same as the number of zero masses. The number of negative β_i (and thus negative eigenvalues) is the same as the number of negative masses (assuming, of course, $h < h_0$).
- (4) There is no restriction on the number of zero and negative masses, as long as the stability condition holds. Our stability proof requires degree of precision is at least zero (see Appendix). If we let $\{1\}^T$ represent a vector with all entries associated with the first degree of freedom at each node equal to 1:

$$\{1\}^T[\tilde{m}_e]\{1\} \geq \rho_{min} vol. (\Omega_e) \neq 0$$

$$\{1\}^T[\tilde{M}]\{1\} \geq \rho_{min} vol. (\Omega) \neq 0$$

where $\Omega_e =$ element e , and $\Omega =$ problem domain, and ρ_{min} is the minimum value of ρ in the appropriate domain. Thus the pathologies of the example of the previous section are ruled out, and elements with nonpositive mass cannot result from stable lumpings.

Next we consider the negative eigenvalues. The worry is that they could lead to unstable modes with low enough frequency to represent mode shapes with significant approximation value. This cannot happen, at least on a fine enough mesh:

Theorem 2: For a stable lumping, given any $N > 0$, there is a sufficiently small $h_0 = h_0(N)$ such that for all $h < h_0$ any $\alpha_i/\beta_i < 0$ satisfies $|\alpha_i/\beta_i| > N$.

Proof: Choose h_0 so that for all $h < h_0$, $[K] + N[\tilde{M}]$ is positive definite. Then $\alpha_i + N\beta_i > 0$, and if $\alpha_i/\beta_i < 0$ this must happen because $\beta_i < 0$ ($\alpha_i \geq 0$). Thus

$$\alpha_i/\beta_i < -N$$

or

$$-\alpha_i/\beta_i > N$$

Corollary 2.1: Under the conditions of Theorem 2 the pencil $[K] - \lambda[\tilde{M}]$ is always regular; that is there are no eigenvalues of the form "0/0".

Proof: In the above proof take $N > 0$ arbitrarily small. $\alpha_i + \beta_i N > 0$. This is a contradiction if $\alpha_i = \beta_i = 0$.

Corollary 2.2: Under the conditions of Theorem 2, there is a complete set of eigenvalues of $[K] - \lambda[\tilde{M}]$, namely, α_i/β_i , $k < i \leq n$ and ∞ (k times).

Remarks:

- (1) Experiments show that the negative eigenvalues are large in magnitude relative to the lower spectrum, even when h is not small.
- (2) The unstable modes due to a negative-weighted lumping formula are always mesh-dependent and are driven higher and higher in frequency with mesh refinement.
- (3) The results of the Theorem and Corollaries flow from stability and the fact that for small enough h , $[K] + N[\tilde{M}]$ can be made positive definite.

This may seem hard to believe in that $N[\tilde{M}]$ adds negative weights to the diagonal of $[K]$. But closer inspection and ref. [6] shows that the diagonal of $[K] + N[\tilde{M}]$ has entries with the following orders of h :

- 1 - D: $[K] = O(1/h)$, $[\tilde{M}] = O(h)$. Thus $\text{diag}([K] - N[\tilde{M}]) \sim O(1/h) \pm O(Nh)$
- 2 - D: $[K] = O(1)$, $[\tilde{M}] = O(h^2)$. Thus $\text{diag}([K] + N[\tilde{M}]) \sim O(1) \pm O(Nh^2)$
- 3 - D: $[K] = O(h)$, $[\tilde{M}] = O(h^3)$. Thus $\text{diag}([K] + N[\tilde{M}]) \sim O(h) \pm O(Nh^3)$.

In the light of the above, the result is less surprising.

Theorem 3: If α is the negative eigenvalue of $K - \lambda[\tilde{M}]$ of smallest magnitude, then given and two real spectral shifts $\lambda_2 > \lambda_1$, which are not eigenvalues and which satisfy one of the following

- (a) $\lambda_1 \geq 0$
- (b) $\lambda_2 < 0$
- (c) $\lambda_2 > 0$ and $\lambda_1 \in (\alpha, 0)$

Then the number of eigenvalues on $[\lambda_1, \lambda_2]$ is the difference between the number of positive members of the signatures of $K - \lambda_1[\tilde{M}]$ and $K - \lambda_2[\tilde{M}]$.

Remarks:

- (1) The proof of Theorem 3 follows directly from the canonical form, equation (22), which has been shown to hold for all stable lumpings.
- (2) Theorem 3 says that a modified Sturm property holds for $K - \lambda[\tilde{M}]$, but two shifts are required to begin.
- (3) The excluded case is $\lambda_2 > 0$, and $\lambda_1 < \alpha$. This can be avoided by using $\lambda_1 = -\epsilon > \alpha$ and varying $\lambda_2 > 0$ to find the positive eigenvalues. If the negative eigenvalues are needed, take $\lambda_2 = -\epsilon$ and vary $\lambda_1 < 0$. In view of Theorem 2, the chances that a "safe" $\epsilon < -\alpha$ cannot be guessed a priori are negligible.

(4) The number of positive members of the required signatures can be computed from the number of sign agreements of the minors [6].

5. ALGORITHMS FOR THE LUMPED EIGENPROBLEM

For vibration analysis and dynamic analysis by modal synthesis, only the lower portion of the spectrum is needed. We have already argued that this portion of the spectrum is as accurate in the optimally lumped case as the consistent case. However, the indefiniteness and/or singularity of the mass matrix does affect the choice of algorithm for the solution of the eigenproblem. Clearly the inverse and/or square root of $[M]$ is no longer available. Lumping in vibration analysis always saves the storage of the upper triangle of $[M]$, which may be significant, but to take full advantage of lumping, solution algorithms should be chosen which, apart from being indifferent to the indefiniteness and/or singularity, display a reduced operation count owing to the diagonal form.

5.1 Algorithms

We have chosen two algorithms which are indifferent to the indefiniteness of $[M]$ and each of which saves essentially a matrix-vector multiplication per iteration owing to the diagonal form of the mass matrix. These algorithms have not been extensively tested, but preliminary numerical tests suggest that they are as robust as their consistent counterparts. In each case, we assume that $h < h_0$ for h_0 sufficiently small to guarantee linear divisors. As pointed out earlier, this has been found to be no real restriction in practice, as the divisors are usually linear with few or even one element. When the divisors are linear, one may easily generalize the standard convergence proofs for each of the algorithms given below.

(1) Inverse iteration

$$([K] - \mu [\tilde{M}]) \{W_{k+1}\} = \gamma_k [\tilde{M}] \{W_k\} \quad (23)$$

where $\{W_k\}$ is the current eigenvector iterate and γ_k is an appropriate normalizing factor [7]. Iteration for one eigenvector at a time, as implied by equation (23) is not the usual finite element practice. Instead block iteration is often employed [6]. This method is greatly enhanced by the use of generalized Jacobi iterations on the pencil $[K_k] - \lambda[M_k]$ obtained by transformation using the current eigenvector iterates at each step. The transformed pencil is not sparse, but approaching closer to a diagonal one at each block iteration; the generalized Jacobi method is more attractive than it would be otherwise in this circumstance. If $[M]$ is rendered indefinite, this could cause problems if the indefiniteness carries over to the transformed matrix, because it does not appear that Jacobi iteration will work if $[M_k]$ is indefinite. We are currently testing the following strategy: shift $[K]$ to make it and each $[K_k]$ positive definite, if necessary, and reverse the role of $[K_k]$ and $[M_k]$ during the Jacobi iterations. The reciprocals of the eigenvalues thus obtained are used where appropriate.

(2) Factored, shifted Lanczos:

Again, if necessary, we shift to make $[K]$ positive definite and exchange the roles of $[K]$ and $[M]$. The Lanczos algorithm is applied in factored form [8,9] to produce a tridiagonal matrix with rows $\{0 \dots \gamma_{i-1} \alpha_i \beta_{i+1} \dots 0\}$:

$$\begin{aligned} [A] &\equiv [K] + \lambda_0 [\tilde{M}] \quad [L][L]^T = [A] \\ \gamma_i [L] \{V_{i+1}\} &= [\tilde{M}] [L]^{-T} \{V_i\} - \alpha_i [L] \{V_i\} - \beta_i [L] \{V_i\} \quad (\beta_1 = 0) \end{aligned} \quad (24)$$

where the Cholesky decomposition is used to obtain $[L]$. The normalization factor, γ_{i-1} can be made equal to β_i by suitable recursive definition of α_i and β_i , so that the resulting tridiagonal matrix is symmetric. The tridiagonal ordinary eigenproblem can be solved any number of ways [10], and the V_i can be saved to reconstruct the original eigenvectors. The attractive feature of this implementation is that the Lanczos algorithm produces all eigenvalues in N iterations in exact arithmetic, but acts as an iterative algorithm for the extreme eigenvalues and vectors requiring very many fewer than N iterates. The extreme eigenvalues at the high end of the spectrum for equation (24) are the reciprocals of the smallest positive eigenvalues of the original shifted pencil, and are precisely the modes we are interested in getting.

There appear to be several other indefinite-indifferent algorithms which save time if the mass matrix is diagonal: one is mentioned in ref. 1. That is the direct conjugate gradient minimization of the square of the Rayleigh quotient [1,11]. This is nearly identical in form to the minimization of the Rayleigh quotient itself (the difference only appears in the scaling of the search direction, which has no practical effect). In fact, a code devised for the consistent case can be modified to take advantage of the diagonal form of $[\tilde{M}]$ and will work otherwise unmodified, even with zero and/or negative masses — as long as some care is exercised in choosing the initial guess. In a number of tests carried out by the first author, the lumped algorithm was unaffected by the poles in the Rayleigh quotient, which are present when the lumped mass matrix is indefinite. The algorithm is nearly twice as fast — half the number of matrix-vector multiplications are required per iteration when compared to the consistent mass matrix algorithm. Furthermore, the lumped algorithm often converged in fewer steps than the consistent algorithm. The algorithm could be defeated only by choosing a singular vector or a vector entirely deficient in the lower modes as an initial iterate. This situation can be entirely avoided by using physical intuition as a guide in the choice of V_0 .

6. TRANSIENT ANALYSIS

In this section we will demonstrate the feasibility and attractiveness of transient analysis by direct time integration using optimally lumped mass matrices. Attention will be restricted to mass matrix lumpings resulting in positive and zero nodal masses* and we will consider, as a model finite element, the 6-node quadratic triangle in which the vertex nodes have zero mass; see Figure 1.

6.1 Partitioned Mixed Integration Schemes

A time integration scheme is constructed by employing a nodal partition consisting of implicit and explicit nodal groups; the implicit nodal group contains all of the zero mass nodes and the explicit group contains all of the positive mass nodes. The partitioned, linear undamped equations of motion become

$$\begin{bmatrix} 0 & & 0 \\ & & \\ 0 & & m^E \end{bmatrix} \begin{Bmatrix} a^I \\ \\ a^E \end{Bmatrix} + \begin{bmatrix} k^{II} & & k^{IE} \\ & & \\ k^{EI} & & k^{LE} \end{bmatrix} \begin{Bmatrix} d^I \\ \\ d^E \end{Bmatrix} = \begin{Bmatrix} p^I \\ \\ p^E \end{Bmatrix} \quad (25)$$

* Research into the stability and accuracy of direct time integration methods for finite element models with indefinite mass matrix lumpings is currently in progress.

where $\{d^I\}$ and $\{a^I\}$ are $(n \times 1)$ vectors and represent implicit approximations to the displacement and acceleration, respectively, and $\{d^E\}$ and $\{a^E\}$ are $(m \times 1)$ vectors and represent explicit approximations to the displacement and acceleration, respectively. In equation (25) and in what follows, there often are corresponding statements on the global and element levels, while some statements — such as those involving global matrix inverses — make sense only on the global level. Since the algorithm presented in this section performs as many operations as possible at the element level, we have opted to use the lower case symbols indicating element level expressions whenever a statement has both global and element level versions, reserving upper case symbols for those statements which make sense only on the global level. The explicit mass matrix, $[m^E]$, is positive definite and the stiffness matrix given by the assemblage of the four partitioned submatrices shown in equation (25) is assumed to be positive semi-definite on the element level, and its assembled global counterpart is assumed to be positive definite because of restraints. This latter restriction on the global stiffness matrix does not seem to be essential but simplifies the analysis. The external force vector is partitioned as $\{p^I\}$ and $\{p^E\}$, the components of which are given on the element level by

$$p_j^e = \int_{\Omega_e} N_I \phi_i(x) d\Omega \quad (26)$$

where N_I is the shape function for node I of element e , $\phi_i(x)$ is either a body force or surface traction in spatial direction i and Ω_e represents element surface or volume depending upon whether ϕ is a traction or body force, respectively; J is the degree-of-freedom number of d.o.f. i at node I . By using the same quadrature rule to evaluate equation (26) as that used in the mass matrix lumping, all of the external loads are lumped into $\{p^E\}$ and $\{p^I\}$ is null.

Numerous combinations of implicit and explicit formulas are possible for the time integration of equation (25). However, because the implicit mass matrix is null, the accuracy and stability of the time integration is directly dependent upon the explicit method that is employed and is independent of the implicit method that is used which simply serves to define the average acceleration and velocity of the massless nodes whose position in time are exclusively dependent upon the position of the adjacent positive mass (explicit) nodes. In particular, we will employ the explicit Newmark formula [12] with $\beta = 0$ and $\gamma = 1/2$, which is similar to central difference, and the implicit Newmark formula with $\beta = 1/4$ and $\gamma = 1/2$, which is identical to the trapezoidal rule (we omit braces enclosing nodal vectors in what follows, whenever it is clear from the context to do so):

$$d_{n+1}^E = d_n^E + \Delta t v_n^E + \frac{\Delta t^2}{2} a_n^E \quad (27)$$

$$v_{n+1}^E = v_n^E + \frac{\Delta t}{2} (a_n^E + a_{n+1}^E) \quad (28)$$

$$d_{n+1}^I = d_n^I + \Delta t v_n^I + \frac{\Delta t^2}{4} [a_n^I + a_{n+1}^I] \quad (29)$$

$$v_{n+1}^I = v_n^I + \frac{\Delta t}{2} [a_n^I - a_{n+1}^I] \quad (30)$$

where subscript n denotes time $n\Delta t$.

Combining equation (27) with (25) and noting that p^I is null if the external forces are lumped using the same quadrature rule as that used in the mass matrix lumping, provides

$$[k^{II}] \{d_{n+1}^I\} = - [k^{IE}] \left\{ d_n^E + \Delta t v_n^E + \frac{\Delta t^2}{2} a_n^E \right\} \quad (31)$$

$$[m^{EE}] \{a_{n+1}^E\} = \{p_{n+1}^E\} - [k^{EI}] \{d_{n+1}^I\} - [k^{EE}] \left\{ d_n^E + \Delta t v_n^E + \frac{\Delta t^2}{2} a_n^E \right\} \quad (32)$$

The computational procedure is shown in Figure 2; for linear problems, its implementation in analysis software with existing stiffness method static analysis and explicit method transient analysis capabilities is straightforward.

Remarks:

- (1) Because the method is partially implicit, it is necessary to form and factor the global stiffness matrix $[K^{II}]$. However, through a suitable node numbering scheme, this matrix has the same size and band structure as that associated with a mesh of an equal number of constant strain triangle finite elements. Thus, the requirements for storage and factorization are considerably less than those usually associated with quadratic triangle finite elements.
- (2) In the implementation shown in Figure 2, two internal force vector evaluations per time step are required. While these evaluations represent the major source of effort per time step, a subsequent example problem will illustrate that it is still very competitive in terms of efficiency.
- (3) These internal force evaluations can be carried out at the element level, as pointed out by the correspondence implied between equations (14) and (15).

6.3 Stability

An important consideration regarding the proposed technique is its numerical stability. Because an explicit method is being employed for the motion of the positive mass nodes, the procedure will be conditionally stable. With typical finite element approximations having positive definite mass matrices, the stability limit for explicit computation is proportional to the reciprocal of the highest natural frequency of the semi-discretization [13] which is strictly mesh dependent and has no physical meaning. In fact, a substantial portion of the upper frequency spectrum is physically meaningless. The effect of a mass quadrature lumping rule that produces positive and zero nodal masses is to force the meaningless portion of the frequency spectrum to infinite; in the proposed scheme the motion at these frequencies is treated implicitly which renders their treatment unconditionally stable. Furthermore, because the remaining portion of the frequency spectrum has been reduced, we expect an improvement in the time step permitted for explicit computation.

1. set initial conditions, $n = 0$, $\{D_0\}$, $\{V_0\} \rightarrow \{A_0\}$
2. compute $\{D_{n+1}^E\} = \{D_n^E\} + \Delta t \{V_n^E\} + \frac{\Delta t^2}{2} \{A_n^E\}$
3. compute $\{D_{n+1}^I\} = -[K^{II}]^{-1} \underbrace{[K^{IE}] \{D_{n+1}^E\}}_{\text{compute element-by-element}}$
4. compute $\{A_{n-1}^I\} = \frac{4}{\Delta t^2} [\{D_{n+1}^I\} - \{D_n^I\} - \Delta t \{V_n^I\}] - \{A_n^I\}$
5. compute $\{A_{n-1}^E\} =$

$$[M^E]^{-1} \left[\{P_{n+1}^E\} - \underbrace{[K^{EI}] \{D_{n+1}^I\} - [K^{EE}] \{D_{n+1}^E\}}_{\text{compute element-by-element}} \right]$$
6. compute $\{V_{n+1}^I\} = \{V_n^I\} + \frac{\Delta t}{2} [\{A_n^I\} + \{A_{n+1}^I\}]$
7. compute $\{V_{n+1}^E\} = \{V_n^E\} + \frac{\Delta t}{2} [\{A_n^E\} + \{A_{n+1}^E\}]$
8. $n \leftarrow n + 1$, go to 2

FIGURE 2

Computational procedure; steps 4 and 6 can be omitted if the velocities and accelerations of the implicit nodes are not of interest.

We define a stable method as one in which a norm of the solution, S , exists at time $n\Delta t$ such that

$$S_n \leq c \quad (33)$$

for all n where c is a nonnegative finite constant [13]; any vector whose norm satisfies equation (33) is said to be bounded. In our analysis of stability, we will employ an energy method similar to [14] in which the conditions required for the satisfaction of equation (33) are deduced. The following definitions are employed

$$\begin{aligned}\hat{d} &= d_{n+1} - d_n \\ \bar{d} &= d_{n+1} + d_n\end{aligned}\quad (34)$$

with similar definitions for the velocity and acceleration difference and sum.

Moving to the global level, the difference of the equation of motion at times $(n+1)\Delta t$ and $n\Delta t$ provides

$$[K^{IE}] \{\hat{D}^E\} - [K^{II}] \{\hat{D}^I\} = \{0\} \quad (35)$$

$$[M^E] \{\hat{A}^E\} - [K^{EE}] \{\hat{D}^E\} + [K^{EI}] \{\hat{D}^I\} = \{0\} \quad (36)$$

where we note that it is sufficient to consider the homogeneous form of equation (25) under our assumption that the external forces are bounded. Premultiplying equation (35) by $\{\hat{V}^E\}^T$ and combining with the explicit formula, Eqs. (27) and (28) provides

$$\{\bar{A}^E\}^T \left[[M^E] - \frac{\Delta t^2}{4} [K^*] \right] \{\hat{A}^E\} + \{\hat{V}^E\}^T [K^*] \{\hat{V}^E\} = 0 \quad (37)$$

where

$$[K^*] = [K^{EE}] - [K^{EI}] ([K^{II}])^{-1} [K^{IE}] \quad (38)$$

Upon rearrangement, equation (37) becomes

$$\begin{aligned}\{A_{n+1}^E\}^T [M^*] \{A_{n+1}^E\} + \{V_{n+1}^E\}^T [K^*] \{V_{n+1}^E\} = \\ \{A_n^E\}^T [M^*] \{A_n^E\} + \{V_n^E\}^T [K^*] \{V_n^E\}\end{aligned}\quad (39)$$

where

$$[M^*] = [M^E] - \frac{4}{\Delta t^2} [K^*] \quad (40)$$

Theorem 4: If $[M^*]$ and $[K^*]$ are positive definite, then $\{A_{n+1}^E\}$ and $\{V_{n+1}^E\}$ are bounded.

Proof: Using induction on equation (39) provides

$$\begin{aligned}\{A_{n+1}^E\}^T [M^*] \{A_{n+1}^E\} + \{V_{n+1}^E\}^T [K^*] \{V_{n+1}^E\} = \\ \{A_0^E\}^T [M^*] \{A_0^E\} + \{V_0^E\}^T [K^*] \{V_0^E\}\end{aligned}\quad (41)$$

and by virtue of equation (28), the theorem follows. ■

Corollary: D_{n+1}^E and D_{n+1}^I are bounded.

Proof: The boundedness of D_{n+1}^E results from equation (27) at the global level, and then the boundedness of D_{n+1}^I results from equation (31) in which it is noted that a sufficient condition for nonsingular $[K^{II}]$ is that the global stiffness matrix is nonsingular. ■

Thus, it only remains to determine the conditions under which the matrices $[K^*]$ and $[M^*]$ are positive definite.

Theorem 5: $[K^*] = [K^{EE}] - [K^{EI}]([K^{II}])^{-1}[K^{IE}]$ is positive definite for arbitrary partitions if the assembled stiffness matrix

$$[K] = \begin{bmatrix} K^{II} & | & K^{IE} \\ \hline K^{EI} & & K^{EE} \end{bmatrix} \quad (42)$$

is symmetric and positive definite.

Proof: Pre- and post-multiply equation (42) by a partitioned vector $\{(X^E)^T | (X^I)^T\}$ where $\{X^E\}$ is $(n \times 1)$ and is nontrivial and $\{X^I\}$ is $(m \times 1)$ and is arbitrary

$$\{X^I\}^T [K^{II}] \{X^I\} + 2 \{X^I\}^T [K^{IE}] \{X^E\} + \{X^E\}^T [K^{EE}] \{X^E\} > 0 \quad (43)$$

For the particular choice $\{X^I\} = -[K^{II}]^{-1}[K^{IE}]\{X^E\}$, equation (43) provides

$$\{X^E\}^T \left[[K^{EE}] - [K^{EI}] ([K^{II}])^{-1} [K^{IE}] \right] \{X^E\} > 0 \quad (44)$$

and the conclusions follow. ■

Thus, the stability of the method depends exclusively upon the positive definiteness of the matrix $[M^*] = [M^E] - \frac{\Delta t^2}{4}[K^*]$. If $(\omega_k^E)^2$ and ψ_k , $k = 1, 2, \dots, n$, are the eigenvalues and vectors corresponding to

$$\left([K^*] - (\omega_k^E)^2 [M^E] \right) \{\psi_k\} = \{0\} \quad (45)$$

then $[M^*]$ can be uncoupled to give the time step size condition for stability

$$\Delta t \leq \frac{2}{\omega_{max}^E} \quad (46)$$

where we refer to ω^E as the explicit frequency, even though it is dependent upon the implicit part of the stiffness matrix as shown in equation (38).

Remarks:

(1) The extreme frequency entering in the stability criterion, equation (46), is based upon a stiffness matrix that is the difference of two positive definite matrices, as shown in equation (38), and a mass matrix, which because of the quadrature lumping rule, has entries of larger magnitude than those associated with more conventional positive definite mass matrix lumpings. Thus, the proposed technique results in a more generous time step restriction than that associated with the exclusive use of an explicit method with a positive definite mass matrix.

(2) Because the eigenproblem given by equation (45) involves a global matrix inversion, the extreme eigenvalue cannot be bounded by the maxima of all unconstrained element frequencies [15]. However, because the second term of equation (38) is positive definite, it is possible to bound the frequency entering in equation (46) by the extreme frequency of the eigenproblem

$$\left([K^{EE}] - (\omega_k^E)^2 [M^E] \right) \{\psi_k\} = \{0\} \quad (47)$$

in which it is noted that the eigenvalue separation theorem [15,16] is applicable.

(3) Because of the definition of $[K^E]$, equation (38), and the particular nodal partition that we are employing (i.e., the implicit nodal group does not occupy a contiguous region of space, but rather is interspersed with the explicit nodal group such that each pair of implicit nodes is separated by an explicit node) the time step restriction given by equation (46) shows that stability is not independent of the part of the stiffness that is treated implicitly. For example, a stiff spring placed between any two implicit nodes in a mesh of quadratic triangle finite elements will adversely affect the timestep restriction.

6.2 Example Problem

In the examples that follow, we will demonstrate the cost effectiveness of the implicit-explicit optimally lumped quadratic displacement triangle element by comparison with an explicit analysis employing a leading competitor element, the 9-node quadratic displacement quadrilateral with optimally lumped mass matrices that are positive definite. Also, the loss of accuracy associated with a particular ad-hoc lumping rule when applied to the quadratic triangle element will be demonstrated by example. All computations were performed on a Harris 800 computer with double precision arithmetic (48 bits per floating point word).

Shown in Figure 3 is a model of a cantilever beam consisting of 40 quadratic displacement triangular finite elements; the material parameters are also listed in the figure. The beam is unloaded and the initial condition consists of the beam at rest except for the free end of the beam (nodes 31-33, 104 and 105) which has a vertical unit step velocity.

Because optimal mass lumping is employed, nodes 1-33 have zero mass and are treated implicitly and nodes 34-105 have positive mass and are treated explicitly. Note that the node numbering scheme is such that the size and band structure of $[K^{II}]$ is minimized. Furthermore, because the explicit matrices $[K^{IE}]$, $[K^{EI}]$ and $[K^{EE}]$ are never assembled, as shown in Figure 2, the efficiency of the explicit phase of the computation is independent of the node numbering scheme.

The maximum time step for stable computation based on an eigenanalysis of the global matrix equations, Eqs. (45) and (46), is $\Delta t \leq 1.93 \times 10^{-6}$ sec. Because the eigenanalysis required to arrive at this result is rather involved, we also consider a more conservative and much easier to compute bound based on an eigenanalysis of the explicit-explicit stiffness matrix only, equation (46), for a single element; this provides $\Delta t \leq 1.84 \times 10^{-6}$ sec. which is conservative by about 5%.

Simulations were performed for a duration of a little more than one fundamental period of vibration and at various time step sizes to validate the stability criteria determined above; computer execution times for these analyses are listed in Table 1.

Results for the two lower time step sizes considered were stable and virtually identical; the vertical displacement time history of the beam tip at the midsurface (node 32) is shown in Figure 4 for the simulation employing the larger step size, $\Delta t = 1.9 \times 10^{-6}$ sec. In order to verify the theoretical stability limit for the method, the simulation was repeated using $\Delta t = 2.0 \times 10^{-6}$ sec. and indeed, the computation was unstable.

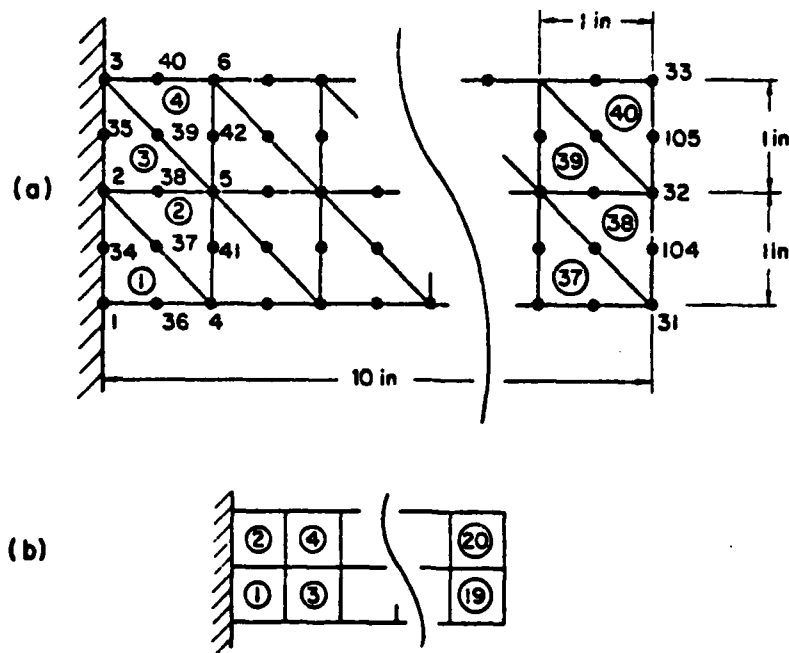


FIGURE 3

Finite element models consisting of 40 quadratic displacement triangle elements (Fig. a) and 20 biquadratic isoparametric elements (Fig. b); material properties: modulus of elasticity = 30×10^6 psi., Poisson's ratio = 0.3 and density = $7.4 \times 10^{-4} \frac{\text{lb} \cdot \text{sec}^{-2}}{\text{in}^4}$.

To show that the method is accurate and cost effective, comparison simulations were performed employing a mesh of 20 bi-quadratic displacement quadrilateral finite elements with optimal mass lumping; see Figure 1. Because the Newton-Cotes formula employed in the mass quadrature has positive weights, the resulting mass matrix is positive definite and a strictly explicit method can be used for the time integration. This is a particularly fair comparison because one quadrilateral element has the same number of degrees-of-freedom and a similar displacement field as a macroelement consisting of two quadratic triangular finite elements. Based upon an eigenanalysis of a single element, the time step restriction was determined to be $\Delta t \leq 1.65 \times 10^{-6}$ sec. Simulations were performed using various time step sizes and for a duration equivalent to that employed for the triangular finite element computations; the computer execution times are given in Table 1 and the vertical displacement time history of the beam tip at the mid-surface (node 32) for the largest stable time step, $\Delta t = 1.7 \times 10^{-6}$ sec., is shown in Figure 4 beside the results for the implicit-explicit optimally lumped triangle element. These results agree extremely well except for a slight period error. Furthermore, a comparison of the execution times for the simulations surprisingly show the implicit-explicit triangular element analysis to be

Quadratic Triangle with Optimal Mass Lumping

$\Delta t (\times 10^{-6} \text{ sec.})$	#steps	execution time (minutes)
1.8	1775	94
1.9	1685	89
2.0	1600	unstable

Quadratic Quadrilateral with Optimal Mass Lumping

$\Delta t (\times 10^{-6} \text{ sec.})$	#steps	execution time (minutes)
1.6	2000	137
1.7	1800	129
1.8	1775	unstable

Quadratic Triangle with Ad-hoc Mass Lumping

$\Delta t (\times 10^{-6} \text{ sec.})$	#steps	execution time (minutes)
1.2	2665	76

TABLE 1

Time step sizes and computer execution times for example problem.

substantially more economical than the explicit quadrilateral element analysis. The reason for this efficiency is threefold: first, the effort required to store and factor $[K^{II}]$ was minimal for this problem. In fact, the size and band structure of this matrix is identical to that for a mesh of 40 constant strain triangular elements. Although the number of equations in $[K^{II}]$ is considerably smaller than the total number of equations (in this example, it has about 30% of the total number of equations) it is noted that its storage and factorization become increasing more inconvenient with increasing problem size. The second source is the fact that fewer time steps are required because of the improved stability, thus, approximately 6% fewer steps were needed. The last source of savings stems from the cost associated with internal force evaluations. Even though the implicit-explicit triangle algorithm requires two internal force evaluations per time step; see Figure 2, as opposed to one for a strictly explicit analysis, the fact that only six integration points per two-triangle macro element are required compared to nine integration points for the quadrilateral, coupled with the fact that the triangle evaluations are easier (fewer multiplications) renders the triangle internal force evaluations slightly more efficient per time step.

In order to demonstrate the importance of using an integration rule of sufficient accuracy in the mass quadrature, we will compare the results obtained by the previous implicit-explicit optimally lumped triangle simulation with an explicit analysis employing

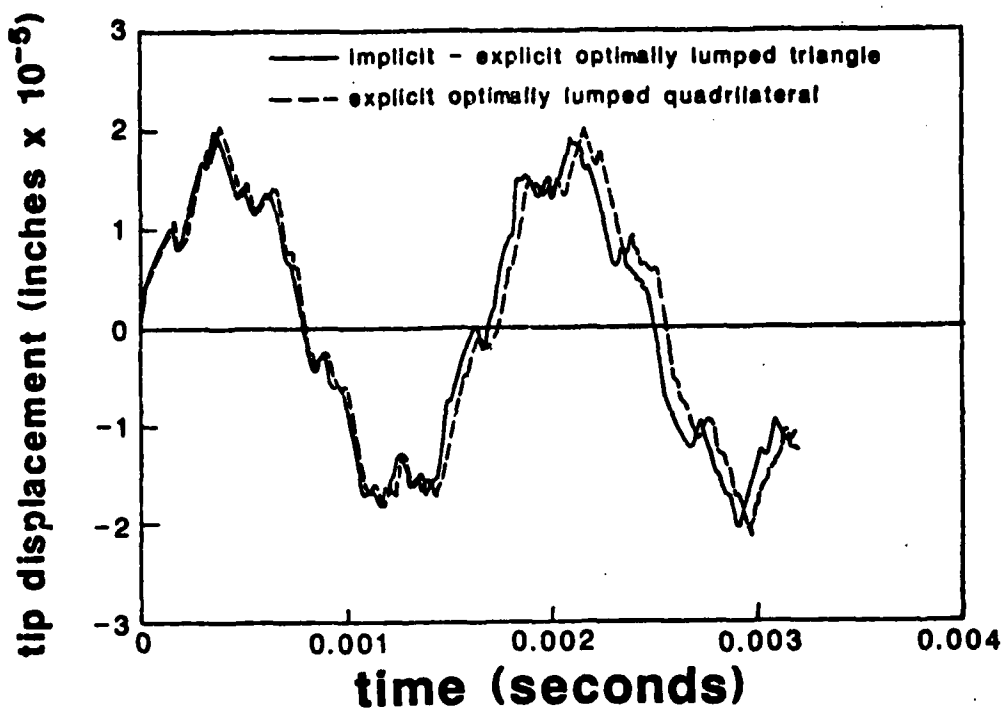


FIGURE 4
Cantilever beam tip displacement time histories for quadratic triangle and biquadratic isoparametric element analyses employing optimal mass lumping.

an identical mesh of quadratic triangle elements with ad-hoc mass lumping to preserve the positive definiteness of the mass matrix. The particular scheme that was employed is detailed in [3], and consists of letting the diagonal entries of the lumped matrix equal the diagonal entries of the consistent mass matrix multiplied by the ratio m/s where m is the total mass of the element and s is the sum of the diagonal entries of the consistent mass associated with translational degrees-of-freedom in one coordinate direction only. The required computer execution time is given in Table 1 and the vertical displacement time history of the beam tip at the mid-surface is shown in Figure 5. Although the phase of the two solutions agree quite well, the amplitudes disagree by as much as 35%. Therefore it is quite apparent that, at least for the particular ad-hoc lumping rule employed in this simulation, that substantial inaccuracies can result from non-optimal mass lumping rules.

7. CONCLUSIONS

We have demonstrated that optimal lumping of masses for higher-order elements can be a viable computational technique, in second-order problems. When only zero masses result from such lumping, we have shown that both vibration and dynamic analyses can be carried out in a manner which is more accurate than an ad-hoc lumping which pre-

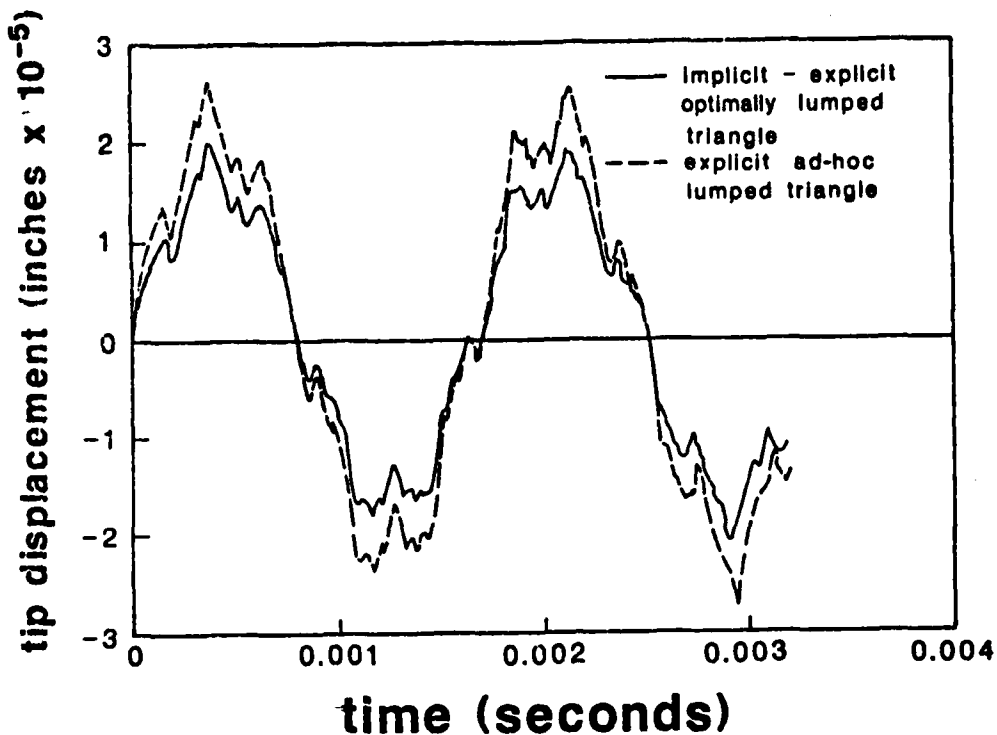


FIGURE 5

Cantilever beam tip displacement time histories for quadratic triangle element analyses employing optimal mass lumping and ad-hoc mass lumping.

serves positive mass, and even more computationally efficient than a widely-used scheme of comparable accuracy which has positive masses. Implicit treatment of the resulting infinite frequencies appears to be a favorable trade-off in dynamic analysis, as long as the number of zero masses is not excessive. We envisage that most of the application of the techniques described here will be in structural and elasto-dynamic problems, but it may be of interest to mention that the motivating example in devising the dynamic algorithm presented here is that of fluid mechanics. There the pressure is in some sense analogous to the modes of infinite frequency introduced by zero masses. It has long been known that the pressure must be treated implicitly in algorithms which treat the velocity explicitly. The reader may have observed that there is a subtle difference with the pressure in incompressible fluid dynamics, however. The pressure at the current iterate of a velocity-explicit Navier-Stokes method must be chosen to make the velocity field weakly divergence-free at the next iterate. The situation here is simpler: the massless nodes, involving modes of infinite frequency, are carried by the stiffness of connected nodes with non-zero mass. As a consequence, the motion of the nodes with nonzero mass is computed first, and the motion of the massless nodes is computed from the motion of the nonzero masses. Such a computational ordering would be unconditionally unstable in fluid mechanics.

In vibration analysis, the infinite frequencies introduced by lumping can be viewed as the setting of some of the inaccurate, high frequency portion of the discrete spectrum to infinite frequency. Heuristically, this is similar to what is done in static condensation, which is equivalent to creating infinite frequencies on a more-or-less ad-hoc basis. Static condensation is likely to lead to reduced accuracy, whereas optimal lumping is guided by rigorous notions of stable and accurate quadrature, and accuracy will not be lost. Of course, optimal lumping will not accomplish the same goal as static condensation, which is to replace all but a few of the most accurate vibration modes by ones with infinite frequency, thereby greatly reducing the dimension of the eigenproblem. It nevertheless appears that optimal lumping can be used in a similar spirit to reduce the computational cost of eigenanalysis. Optimal lumping may also be viewed as a means of pushing to the limit the notion of modifying the upper portion of the discrete spectrum without suffering an accuracy loss.

This finally brings us to the question of negative masses. In spite of first appearances to the contrary, we have shown that they do not interfere with vibration analysis. We like to think of the negative masses as ones that have been forced to even "higher than infinite" frequency by the lumping scheme, though this may only be a somewhat quaint descriptive analogy. There should be a very real doubt about the dynamical viability of negative masses; they introduce high frequency, unconditionally unstable modes into the problem, which seems the last thing anyone would want to do in dynamic analysis. We do not believe it is as bad as that; the saving grace may lie in the fact we have established here: the negative masses give rise to very high frequency modes. This portion of the spectrum is just the one subject to algorithmic damping by many good integrators. To put it another way, many ODE integrators have stable regions which include substantial portions of the right half plane (backwards Euler's method, for one, though we are not recommending it as a practical method). We are currently investigating the possibility of devising time-stepping procedures with sufficient algorithmic damping to be indifferent to spurious unstable modes introduced by optimal lumpings with negative masses.

8. REFERENCES

1. I. Fried and D. S. Malkus, Finite element mass matrix lumping by numerical integration with no convergence rate loss, *Int. J. Solids and Struct.* **11**, 461-466(1975).
2. G. H. Golub, Some modified matrix eigenvalue problems, *S. I. A. M. Review* **15**, 318-334(1973).
3. R. D. Cook, *Concepts and Applications of Finite Element Analysis*, Wiley, New York, 1974.
4. F. R. Gantmacher, *Matrix Theory*, Vol. II, Chelsea, New York, 1971.

5. G. Fix, Effects of quadrature errors in finite element approximation of steady state eigenvalue and parabolic problems, pp. 525-556, in *Mathematical Foundations of the Finite Element Method*, I. Babuska and A. K. Aziz, eds., Academic Press, New York, 1972.
6. K. J. Bathe. *Finite Element Procedures in Engineering Analysis*. Prentice-Hall, Englewood Cliffs, 1982.
7. G. Peters and J. H. Wilkinson. $Ax = \lambda Bx$ and the generalized eigenproblem, *S. I. A. M. J. Numer. Anal.* **7**, 479-492(1970).
8. C. C. Paige. Computational variant of the Lanczos algorithm for the eigenproblem, *J. Inst. Maths. Applics.* **10**, 373-381(1972).
9. G. Golub, R. Underwood, and J. H. Wilkinson, The Lanczos algorithm for the symmetric $Ax = \lambda Bx$ problem, Stanford University Computer Science Department Report STAN-CS-72-270(1972).
10. J. H. Wilkinson, *The Algebraic Eigenvalue Problem*, Clarendon Press, Oxford, 1965.
11. I. Fried, Optimal gradient minimization scheme for finite element eigenproblems, *J. Sound Vib.* **20**, 333-342(1972).
12. N. M. Newmark, A method of computation for structural dynamics, *J. Eng. Mech. Div. A. S. C. E.* **85**, 67-94(1959).
13. R. D. Richtmeyer and K. W. Morton, *Difference Methods for Initial Value Problems*, Interscience, New York, 1967.
14. T. J. R. Hughes and W. K. Liu, Implicit-explicit finite elements in transient analysis: Stability theory, *J. Appl. Mechs.* **45**, 371-374(1978).
15. T. Belytschko and T. J. R. Hughes, *Computational Methods for Transient Analysis*, Vol. I in *Computational Methods in Mechanics*, North-Holland, Amsterdam, 1983.
16. I. Fried, Bounds on the extremal eigenvalues of the finite element stiffness and mass matrices and their spectral condition number, *J. Sound Vib.* **22**, 407-418(1972).
17. P.G. Ciarlet, *The Finite Element Method for Elliptic Problems*, North-Holland, Amsterdam, 1978.

APPENDIX

Sharpening of G. Fix's result [5]* on quadrature errors when $\tilde{a}(\cdot, \cdot) = a(\cdot, \cdot)$. Following ref. 5, element-by-element quadrature errors are of the form (applied to scalar component of \mathbf{u}^h , call it u^h):

$$h^{\ell_0} \int_e D^\gamma (u^h v^h)' dV; \quad |\gamma| = \gamma_1 + \gamma_2 = \ell_0 \quad (\text{A.1})$$

where γ = typical derivative multi-index. ℓ_0 = degree of lowest order polynomial not integrated exactly. We assume, as does ref. 5, that the inverse inequality

$$|D^{\alpha_0} u^h|_{0,e} \leq \frac{C}{h} \|u^h\|_{0,e}; \quad |\alpha_0| = 1 \quad (\text{A.2})$$

on each element. There are two cases. (A) Stability: u^h and v^h are arbitrary trial functions and (B) accuracy: u^h is the f.e.m. solution and v^h is an arbitrary trial function. In case (B) for $0 \leq s \leq p$

$$\sum_e \|u^h\|_{s+1,e} \leq C \|u\|_{p+1}^2 \quad (\text{A.3})$$

where u is the exact solution. The left-hand side sums to $\|u^h\|_s$ for $s = 0$ or 1 .

Case A: (A.1) is the sum of terms of the form

$$E_e = Ch^{\ell_0} \int_e |(D^\alpha u^h) (D^\beta v^h)| dV; \quad |\alpha| + |\beta| = |\gamma| = \ell_0 \quad (\text{A.4})$$

Suppose $|\alpha| \neq 0$ and $|\beta| \neq 0$, then

$$E_e \leq Ch^{\ell_0} \|D^\alpha u^h\|_{0,e} \|D^\beta v^h\|_{0,e} \leq C_e h^{\ell_0} \frac{\|D^{\alpha_0} u^h\|_{0,e}}{h^{|\alpha|-1}} \frac{\|D^{\beta_0} v^h\|_{0,e}}{h^{|\beta|-1}}$$

where $|\alpha_0| = |\beta_0| = 1$. Thus

$$E_e \leq C_e h^{\ell_0 - |\alpha| - |\beta| + 2} \|u^h\|_{1,e} \|v^h\|_{1,e} = C_e h^2 \|u^h\|_{1,e} \|v^h\|_{1,e} \quad (\text{A.5})$$

Now

$$\begin{aligned} & \sum_e \left| \int_e D^\gamma (u^h v^h) dV \right| \\ & \leq \sum_e |E_e| \leq h^2 \left(\sum_e \|u^h\|_{1,e}^2 \right)^{\frac{1}{2}} \left(\sum_e \|v^h\|_{1,e}^2 \right)^{\frac{1}{2}} = Ch^2 \|u^h\|_1 \|v^h\|_1 \end{aligned} \quad (\text{A.6})$$

* Reference numbers in the Appendix refer to the Reference section of the main body of the paper.

If either $|\alpha| = 0$ or $|\beta| = 0$, then the following case is representative:

$$h^{\ell_0} \int_e (D^\gamma u^h) v^h dV \leq \|D^\gamma u^h\|_{-1,e} \|v^h\|_{1,e} \quad (\text{A.7})$$

and

$$\begin{aligned} \|D^\gamma u^h\|_{-1,e} &= \sup_{w \in H_0^1(e)} \|w\|_{1,e}^{-1} \int_e (D^\gamma u^h) w dV \\ &= \sup_{\|w\|_{1,e} = 1} \left[- \int_e (D^{\gamma'} u^h) (D^{\gamma_0} w) dV \right] \end{aligned}$$

where $|\gamma'| = \ell_0 - 1$, $|\gamma_0| = 1$. Now

$$\begin{aligned} &\int_e (D^{\gamma'} u^h) D^{\gamma_0} w dV \\ &\leq \|D^{\gamma'} u^h\|_{0,e} \|D^{\gamma_0} w\|_{0,e} \leq \frac{C}{h^{|\gamma'| - 1}} \|u^h\|_{1,e} \|D^{\gamma_0} w\|_{0,e} \leq \frac{C'}{h^{|\gamma'| - 1}} \|u^h\|_{1,e} \end{aligned}$$

Thus

$$h^{\ell_0} \left| \int_e (D^\gamma u^h) v^h dV \right| \leq C_e h^2 \|u^h\|_{1,e} \|v^h\|_{1,e}$$

and summing as before shows in general that

$$|b(u^h, v^h) - \tilde{b}(u^h, v^h)| \leq Ch^2 \|u^h\|_1 \|v^h\|_1 \quad (\text{A.8})$$

where $b(\cdot, \cdot)$ refers to the L_2 inner product in one vector component of the trial spaces defined in the main body of the paper. Since the same interpolations and quadratures are used in each component, the result of equation (A.8) carries over to $b(u^h, v^h)$; this proves stability.

Remarks:

1. Fix's result can be sharpened because $b(\cdot, \cdot)$ involves no derivatives. One derivative "on each side" must be left behind to compare to $\|\cdot\|_1$, hence two fewer powers of h are lost in the process.
2. When all ℓ_0 derivatives are on one side, one must be "moved over". The negative norm argument is just a compact way of applying the divergence theorem and arguing away the boundary integral.
3. The above argument shows that any quadrature formula with degree of precision ≥ 0 is stable for $b(\cdot, \cdot)$. Accuracy is another matter.

Case B: We argue that (A.1) is small indirectly, making use of (A.3). Assume that a non-conforming triangle of (complete) degree $0 \leq q \leq p$ can be inscribed in every element

of the mesh, and that the conditions on the mesh are such that the standard error analysis [17] applies to elements, so that if \tilde{u}^h is a standard approximation to u^h from the implied space of complete (discontinuous) polynomials

$$\|u^h - \tilde{u}^h\|_{1,e} \leq C_e h^q \|u^h\|_{q+1,e} \quad (\text{A.9})$$

Note that $q = 0$ is allowed giving only boundedness of the left-hand side. Further let us assume that $\tilde{b}(\tilde{u}^h, v^h) = b(\tilde{u}^h, v^h)$ (whereas $\tilde{b}(u^h, v^h)$ may differ from $b(u^h, v^h)$). Then

$$\begin{aligned} b(u^h, v^h) - \tilde{b}(u^h, v^h) &= b(u^h - \tilde{u}^h, v^h) - \tilde{b}(u^h - \tilde{u}^h, v^h) = \\ &= \rho \int_{\Omega} (u^h - \tilde{u}^h) v^h dV - \rho \sum_{\epsilon} \sum_k u_k^{\epsilon} (u^h - \tilde{u}^h)_k v_k^h \\ &\leq \sum_{\epsilon} C_e h^{q+2} \|u^h\|_{q+1,e} \|v^h\|_{1,e} = \sum_{\epsilon} C_e h^{q+2} \|u^h\|_{q+1,e} \|v^h\|_{1,e} \end{aligned}$$

where the inequality is determined from the assumption of stability. The subscript k refers to function value at the k^{th} quadrature point. Note we assume $\rho = \text{constant}$; the result will apply when ρ is a smoothly varying coefficient [17]. We accumulate the error as in equation (A.6), and finally arrive at the desired result:

$$|b(u^h, v^h) - \tilde{b}(u^h, v^h)| \leq C h^{q+2} \|u\|_{p+1} \|v^h\|_1 \quad (\text{A.10})$$

Remarks:

1. For the bilinear element, $q = 0$, leads to $\tilde{b}(\tilde{u}^h, v^h) = b(\tilde{u}^h, v^h)$, thus the entire solution is $O(h)$ (optimally) accurate [5]. For the biquadratic element, $q = 0$ or 1 leads to $O(h^2)$, which is also optimal.
2. $Bi - p$ polynomials have a power of h to spare. With linear, quadratic and cubic triangles the exact integration condition cannot be met unless $q = 0, 0$ and 1 resp.
3. All elements discussed in the body of the paper lead to recovery of full accuracy by allowing $p - q \leq 2$.

REPORT DOCUMENTATION PAGE		READ INSTRUCTIONS BEFORE COMPLETING FORM
1. REPORT NUMBER 2915	2. GOVT ACCESSION NO.	3. RECIPIENT'S CATALOG NUMBER
4. TITLE (and Subtitle) ZERO AND NEGATIVE MASSES IN FINITE ELEMENT VIBRATION AND TRANSIENT ANALYSIS		5. TYPE OF REPORT & PERIOD COVERED Summary Report - no specific reporting period
		6. PERFORMING ORG. REPORT NUMBER
7. AUTHOR(s) David S. Malkus and Michael E. Plesha		8. CONTRACT OR GRANT NUMBER(s) DAAG29-80-C-0041
9. PERFORMING ORGANIZATION NAME AND ADDRESS Mathematics Research Center, University of 610 Walnut Street Wisconsin Madison, Wisconsin 53705		10. PROGRAM ELEMENT, PROJECT, TASK AREA & WORK UNIT NUMBERS Work Unit Number 3 - Numerical Analysis and Scientific Computing
11. CONTROLLING OFFICE NAME AND ADDRESS U. S. Army Research Office P. O. Box 12211 Research Triangle Park, North Carolina 27709		12. REPORT DATE February 1986
		13. NUMBER OF PAGES 27
14. MONITORING AGENCY NAME & ADDRESS (if different from Controlling Office)		15. SECURITY CLASS. (of this report) UNCLASSIFIED
		15a. DECLASSIFICATION/DOWNGRADING SCHEDULE
16. DISTRIBUTION STATEMENT (of this Report) Approved for public release; distribution unlimited.		
17. DISTRIBUTION STATEMENT (of the abstract entered in Block 20, if different from Report)		
18. SUPPLEMENTARY NOTES		
19. KEY WORDS (Continue on reverse side if necessary and identify by block number) Explicit Numerical quadrature Finite element Stability Implicit Time integration Lumping Vibration modes Mass matrix		
20. ABSTRACT (Continue on reverse side if necessary and identify by block number) Mass matrix lumping by quadrature is considered. Accuracy requirements seem to dictate the use of zero or negative masses for multi-dimensional higher-order elements. It is shown that the zero and/or negative masses do not destroy the essential algebraic properties of the discrete eigenproblem, in spite of the negative or infinite eigenvalues which may result. Explicit transient methods require positive definite lumping which, for some elements, may only be achieved by sacrificing accuracy to avoid the negative or zero masses that would render the lumping indefinite. An implicit-explicit time		

20. ABSTRACT - cont'd.

integration method based on quadratic triangles with optimal lumping is devised, analysed, and tested. It treats the nodes with nonzero masses explicitly and the nodes with zero masses implicitly. Analysis and numerical tests show that this formulation is optimally accurate and less costly than a similar method with nonzero masses, based on optimally lumped biquadratic rectangles. The method is also found to be substantially more accurate than the fully explicit method based on lumping the triangular elements in an ad-hoc fashion to retain non-zero masses.

END

DTIC

6-86